

Alterations in glycolytic/cholesterogenic gene expression in hepatocellular carcinoma

Jianwen Jiang^{1,2,3,4,*}, Qiuxian Zheng^{4,5,*}, Weiwei Zhu^{2,3,*}, Xinhua Chen^{2,3,4}, Haifeng Lu^{4,5}, Deying Chen^{4,5}, Hua Zhang^{4,5}, Min Shao¹, Lin Zhou^{2,3}, Shusen Zheng^{2,3}

¹Department of Health Management, The First Affiliated Hospital, Zhejiang University School of Medicine, Hangzhou 310003, China

²Department of Hepatobiliary and Pancreatic Surgery, The First Affiliated Hospital, Zhejiang University School of Medicine, Hangzhou 310003, China

³Key Laboratory of Combined Multi-Organ Transplantation, Ministry of Public Health, The First Affiliated Hospital, Zhejiang University School of Medicine, Hangzhou 310003, China

⁴Collaborative Innovation Center for Diagnosis and Treatment of Infectious Diseases, The First Affiliated Hospital, Zhejiang University School of Medicine, Hangzhou 310003, China

⁵State Key Laboratory for Diagnosis and Treatment of Infectious Diseases, The First Affiliated Hospital, Zhejiang University School of Medicine, Hangzhou 310003, China

*Equal contribution

Correspondence to: Shusen Zheng, Jianwen Jiang; **email:** shusenzheng@zju.edu.cn, jiangjw@zju.edu.cn

Keywords: hepatocellular carcinoma, metabolic classification, glycolysis, cholesterogenic, molecular mechanism

Received: February 27, 2020

Accepted: April 20, 2020

Published: June 1, 2020

Copyright: Jiang et al. This is an open-access article distributed under the terms of the Creative Commons Attribution License (CC BY 3.0), which permits unrestricted use, distribution, and reproduction in any medium, provided the original author and source are credited.

ABSTRACT

Metabolic reprogramming is a hallmark of tumors, including hepatocellular carcinoma (HCC). We used data from The Cancer Genome Atlas and the International Cancer Genome Consortium to assess the alterations in glycolytic and cholesterogenic genes in HCC and to determine their association with clinical features in HCC patients. Based on the gene expression profiles from these databases, we established four subtypes of HCC: cholesterogenic, glycolytic, mixed, and quiescent. The prognosis of the cholesterogenic subgroup was poorer than that of the glycolytic group. Tumors in the glycolytic group were more sensitive to chemotherapy. We also explored the relationships between these metabolic subtypes and previously established HCC subgroups. Glycolytic gene expression correlated strongly with poorer prognostic gene expression in the Hoshida classification of HCC. Whole-genome analyses indicated that aberrant amplification of *TP53* and *MYC* in HCC were associated with abnormal anabolic cholesterol metabolism. The mRNA levels of mitochondrial pyruvate carriers 1 and 2 differed among the HCC metabolic subtypes. In a bioinformatics analysis we identified genomic characteristics of tumor metabolism that varied among different cancer types. These findings demonstrate that metabolic subtypes may be valuable prognostic indicators in HCC patients.

INTRODUCTION

Hepatocellular carcinoma (HCC) is the most common type of primary liver cancer, accounting for 70-90% of cases [1]. The occurrence of HCC is strongly associated with hepatitis viral infections, alcohol abuse and aflatoxin contamination [2]. Because HCC is difficult to diagnose early, and is also highly malignant and

insensitive to chemoradiotherapy, it is a serious threat to human health. The latest epidemiological surveys have demonstrated that HCC is the second leading cause of cancer death among men worldwide and the sixth leading cause of cancer death among men in developed countries [3, 4]. Although advances in HCC treatment have been made in recent years, HCC recurrence and metastasis are still key determinants of the long-term

prognosis of patients, and are the main obstacles to patient survival [5].

The study of metabolic reprogramming in tumors has developed in recent years, and may provide a new method of eliminating tumor cells effectively [6, 7]. To satisfy the additional energy requirements for their proliferation and growth, tumor cells must reshape their metabolic pathways [8]. Tumor cells differ from normal cells in their metabolism of glucose, amino acids, fatty acids and nucleotides, which provide large amounts of energy and intermediates [9]. The metabolic reprogramming of tumor cells primarily involves hyperactive glycolysis and fatty acid synthesis. Key metabolic enzymes are upregulated in a variety of cancer types, including lung cancer [10], prostate cancer [11], kidney cancer [12] and lymphoma [13]. Using an online prediction tool, we previously illustrated that beta-lactamase expression correlated strongly with the expression of genes involved in lipid metabolism in HCC patients [14]. Although disruptions in certain signaling pathways are known to contribute to metabolic reprogramming in cancer, alterations in glycolipid metabolism have rarely been reported in liver cancer.

Otto Warburg first reported that liver cancer cells exhibited significantly greater glycolytic activity than normal hepatocytes, and proposed that rapidly proliferating tumor cells were powered by aerobic glycolysis [15]. This phenomenon has been observed in different tumor types, and has become fundamental to our understanding of tumor metabolism. Similarly, cholesterol levels are significantly higher in liver cancer than in healthy liver tissues [16]. Cholesterol is important for the formation of cell membranes and for the synthesis of bile acids, vitamin D and steroid hormones [17]. Previous studies have revealed that metabolism-related genes (including isoenzymes within specific pathways) exhibit an increased mutation rate in cancer patients and display heterogeneity among different cancer types [18, 19]. However, no systematic reports have been published to date on the relationship of abnormal glucose and lipid metabolism to the molecular mechanism, prognosis and treatment of HCC.

The lack of molecular subtyping for HCC tumors makes it impossible to screen patients for their suitability for targeted therapies. The latest guidelines for the diagnosis of primary liver cancer mainly describe its pathology in terms of gross and histological morphology, while only using immunohistochemical indexes to distinguish the source of the tumor cells (HCC, biliary cell carcinoma or mixed cell types). The molecular classification of liver cancer lags behind those of lung, breast and gastric cancers, and does not

satisfy the requirements for clinically accurate treatment. Understanding the reprogramming of energy metabolism in liver cancer could provide a new strategy for subtyping HCC patients so that precise and targeted treatments can be developed to improve survival.

In the present study, we classified HCC patients into different subtypes based on their expression of genes involved in glycolysis and cholesterol synthesis. We explored the differences in survival and other clinical characteristics among the various metabolic subtypes of HCC, and identified carcinogenic molecular events in the different subtypes. We now propose a clinically feasible HCC-typing scheme, which may become a new tool to guide the targeted therapy of HCC.

RESULTS

Four metabolic subgroups of HCC were identified based on the dual analysis of glycolytic and cholesterologenic gene expression

In total, 610 HCC tumor samples were included in this study (The Cancer Genome Atlas [TCGA], $n = 373$, and International Cancer Genome Consortium [ICGC], $n = 237$). Samples with $< 30\%$ were excluded. Reactome gene set enrichment analysis was applied to obtain the “glycolysis” ($n = 29$) and “cholesterol biosynthesis” ($n = 72$) gene sets. Unsupervised consensus clustering analysis was implemented to classify the two subgroups of significantly expressed glycolytic ($n = 9$) and cholesterologenic ($n = 11$) genes for further metabolic subtyping (Figure 1A).

We calculated the median levels of glycolytic and cholesterol-producing genes in each sample. Based on the co-expression of the two gene sets, we separated the gene profiles into four metabolic subtypes of HCC: the glycolytic subgroup (high expression of glycolytic genes and low expression of cholesterol synthesis genes), cholesterologenic (high expression of cholesterol synthesis genes and low expression of glycolytic genes), mixed (high expression of both cholesterol synthesis genes and glycolytic genes) and quiescent (low expression of both cholesterol synthesis genes and glycolytic genes) subgroups (Figure 1B). The levels of genes involved in glycolysis and cholesterol synthesis are illustrated in Figure 1C, along with the proportion of patients in each metabolic subgroup. The quiescent phenotype group contained the largest number of patients (332/610, 54.4%), followed by the cholesterologenic (164/610, 26.9%), glycolytic (65/610, 11%) and mixed subtypes (49/610, 8%).

To determine the relationship between the HCC metabolic subgroup and patient prognosis, we

performed a statistical cluster analysis on HCC metabolic oncogene characteristics in metastatic and non-metastatic patients. There was no significant difference in the distribution of the metabolic subgroups between the metastatic and non-metastatic groups. However, there were significant differences in overall survival based on cholesterol-generating and glycolytic gene expression. The clinical outcomes were significantly worse in the cholesterol-generating subgroup than in the glycolytic group ($p = 0.017$) (Figure 1D). In both the non-metastatic and metastatic groups of HCC patients (Figure 1E and 1F, $p = 0.049$ and $p = 0.027$, respectively), there was a significant difference in survival between the cholesterogenic and glycolytic subgroups. Surprisingly, survival benefits were observed in patients with increased expression of glycolytic genes. These findings indicated that there are metabolic phenotypes associated with glycolysis/cholesterogenesis and prognosis in HCC.

Relationship between the tumor genome metabolic subtype and the HCC subtype

Metabolic reprogramming is now accepted as a hallmark of cancer [20, 21], and we found significant abnormalities in metabolic gene expression in HCC patients. We next investigated the frequency of single nucleotide variations (SNVs), insertion-deletion mutations (INDELs) and copy number variations (CNVs) [22] in genes associated with the different metabolic subtypes of liver hepatocellular carcinoma (LIHC) cohorts (Figure 2A). The mutational frequency of each gene did not differ significantly among the subtypes (Fisher's exact test and Benjamini-Hochberg (BH) test-corrected, $p > 0.05$ after correction). However, the median levels of cholesterol synthesis genes were significantly greater in *MYC*-amplified and *TP53*-deleted samples than in samples without these alterations (Figure 2B). Cholesterogenic gene expression correlated positively with *MYC* mutations ($p = 0.039$, $R = 0.1$) (Figure 2C) and negatively with *TP53* mutations ($p = 0.037$, $R = -0.14$) (Figure 2D). These findings are consistent with the high mutational frequency of *TP53* and *MYC*, and support the notion that mutations in *TP53* and *MYC* promote tumor progression by inducing abnormal glucose utilization. Thus, tumors may be vulnerable to changes in glycolysis.

The relationship between survival-related features and gene expression in HCC has been illustrated in previous studies [23, 24]. Hoshida's classification, Budhu's metastasis-averse/inclined microenvironment (MAM/MIM) and Chew's classification have been used to classify liver cancer according to the clinical prognosis (see Methods for details) (Supplementary

Table 1). To explore the association between the glycolytic/cholesterogenic metabolic phenotypes and the tumor subtypes from the above-mentioned prognostic classification methods, we identified the tumor subtype and metabolic phenotype of each sample (Figure 3A). Most of the patients in the quiescent group had favorable prognoses according to the Hoshida classification (75.4%), while fewer patients in the mixed group (29.9%, adjusted $p = 0.0025$) and the cholesterogenic group (34.8%, adjusted $p = 0.022$) had favorable prognoses (Figure 3B). The number of MAM/MIM samples according to the Budhu classification differed significantly between the quiescent group and the mixed group. The number of samples with a poor prognosis according to the Chew classification differed significantly between the quiescent group and the glycolytic group.

We also analyzed the correlation of cholesterogenic/glycolytic gene expression with prognostic gene expression according to the Hoshida classification. The expression of genes associated with a poor prognosis correlated positively with the expression of genes in the cholesterol synthesis pathway. Likewise, the expression of genes associated with a good prognosis correlated negatively with the expression of genes in the cholesterol synthesis pathway. Glycolytic gene expression correlated positively with prognostic gene expression in both the better and poorer prognosis groups, but the correlation was stronger in the poorer prognosis group (Figure 3C). This was consistent with the significant association between cholesterogenic gene expression and a poorer survival prognosis. These data indicated that glycolysis and cholesterol synthesis are potential metabolic targets in patients with different HCC subtypes.

Mitochondrial pyruvate carrier complex expression differed among the metabolic subtypes

The mitochondrial pyruvate carrier (MPC) complex in the inner membrane of the mitochondria transfers free pyruvate from the cytoplasm to the mitochondrial matrix [25]. Previous studies observed that MPC1 and MPC2 were different in metabolic pathways and promoted tumor glycolysis activity. This difference is important in lactic acid production [26, 27].

To explore the association of *MPC1* and *MPC2* with the different metabolic phenotypes, we assessed the metabolic subpopulations for SNVs, INDELs, CNVs and mRNA expression changes in these genes. The CNVs in *MPC1* and *MPC2* differed significantly among the metabolic subgroups; however, the CNVs in *MPC1* were deletions in almost all of the HCC samples, while the CNVs in *MPC2* were mostly amplifications

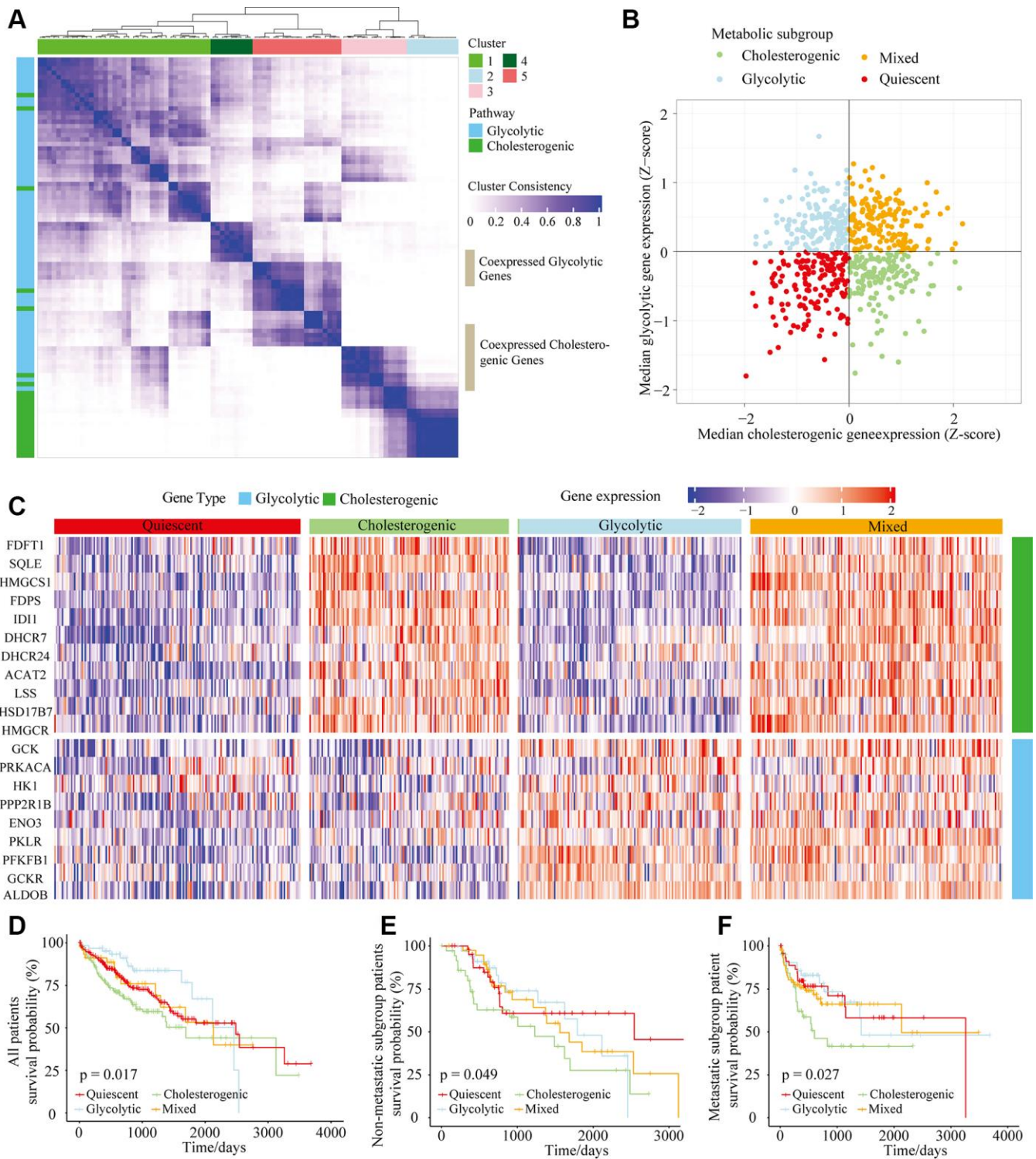


Figure 1. The metabolic gene landscape of HCC based on glycolytic and cholesterogenic clusters. (A) Heat map of consensus clustering ($k=5$) for glycolytic and cholesterogenic genes in resected and metastatic LIHC samples ($n=610$). (B) Scatter plot of the median levels of co-expressed glycolytic (x-axis) and cholesterogenic (y-axis) genes in each LIHC sample. Metabolic subgroups were assigned based on the relative levels of glycolytic and cholesterogenic genes. (C) Heat map of differential gene expression patterns in glycolytic and cholesterogenic gene clusters across subgroups. (D) Kaplan-Meier survival analyses of patients with all subtypes of LIHC; the log-rank test p value is shown. (E) Overall survival analyses in the metastatic subgroup of LIHC patients; the log-rank test p value is shown. (F) Overall survival analyses in the non-metastatic LIHC cohort; the log-rank test p value is shown.

(Figure 4A). *MPC1* and *MPC2* mRNA levels differed significantly among the metabolic subgroups. *MPC2* expression was significantly lower in the glycolytic group than in the other groups, whereas *MPC1* expression was significantly greater in the glycolytic group. *MPC2* expression was significantly higher in the cholesterogenic group than in the quiescent group (Figure 4B). Thus, the dysregulation of mitochondrial pyruvate transport at the mRNA level may be associated with the metabolic tumor subtypes.

To find cellular pathways associated with *MPC1/2* expression, we performed a comprehensive correlation analysis between *MPC1/2* and all the other tested genes ($n = 25,483$). In total, 168 genes correlated positively with *MPC1/2*, while 14 genes correlated negatively with *MPC1/2* (Spearman correlation BH-corrected $p < 0.01$) (Figure 4C). The positively correlated genes were associated with extracellular matrix function (hypergeometric test, BH regulation $p < 0.05$). The pathways enriched in the negatively correlated genes

were involved in carbon chain binding and phosphorylation (Figure 4D). These data suggested that *MPC1* and *2* participate in cellular networks associated with tumor progression in HCC.

Correlation between glycolytic and cholesterogenic gene expression in various cancers

It is very important to identify cancers that have unique metabolic characteristics driven by their mutational environment and organ-specific enzyme expression [28]. To identify the dysregulated routes of metabolism in different cancers, we performed cluster analyses of glycolytic and cholesterogenic gene expression in 26 cancer types (tumor content $\geq 30\%$) from TCGA (Supplementary Table 2). Gene co-expression pathway-specific profiles and hub genes were identified via network topology analysis in 13 cancer types. Metabolism-related genes were co-expressed in most tumor types. However, due to the differential co-expression of glycolytic and cholesterogenic genes,

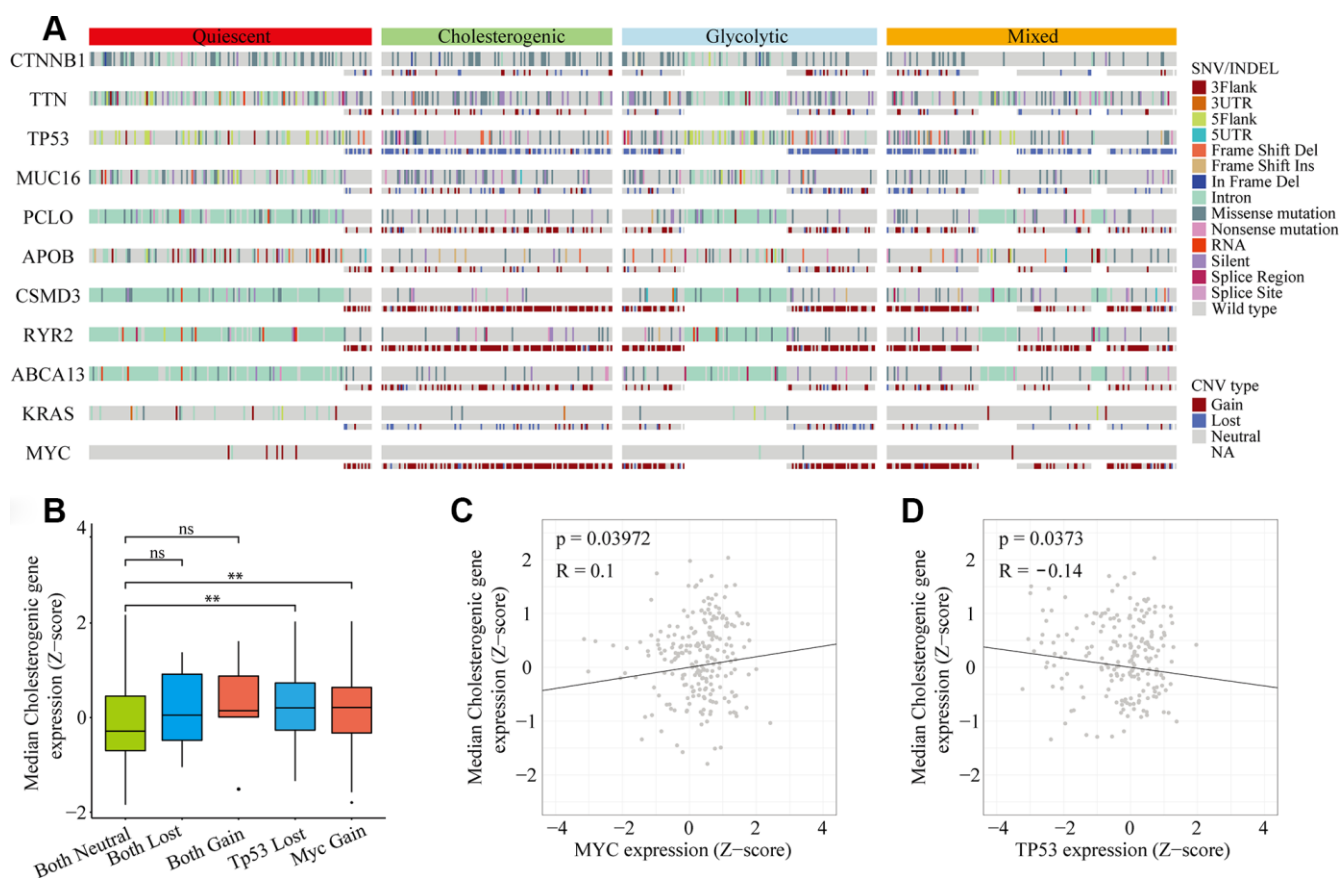


Figure 2. Gene mutational landscape across metabolic subgroups of HCC. (A) OncoPrint analysis indicating the distribution of SNVs, INDELS and CNVs of frequently mutated genes in LIHC across the metabolic subtypes. **(B)** Box plot of the median expression of cholesterogenic genes in samples with CNVs in *TP53* and/or *MYC*. **(C)** Scatter plot of the correlation between the median cholesterogenic gene expression and *MYC* expression. **(D)** Scatter plot of the relationship between the median cholesterogenic gene expression and *TP53* expression.

some genes were only co-expressed in a few cancer types, indicating that certain genes contribute to the tumor metabolic program in a cell-type-specific manner (Figure 5A). Cholesterogenic gene expression correlated positively with poor prognostic gene expression in the Hoshida classification system, not only in HCC (Spearman correlation BH-corrected $p < 0.05$), but also in a range of other tumor types (Figure 5B). For some cancers, the median cholesterogenic gene expression correlated positively with *KRAS* expression (cervical squamous cell carcinoma [CESC],

glioblastoma multiforme [GBM], kidney renal clear cell carcinoma [KIRC], brain lower grade glioma [LGG], lung squamous cell carcinoma [LUSC], ovarian serous cystadenocarcinoma [OV], pancreatic adenocarcinoma [PAAD], pheochromocytoma and paraganglioma [PCPG], prostate adenocarcinoma [PRAD] and stomach adenocarcinoma [STAD]) or *MYC* expression (PCPG, STAD and LUSC) (BH-corrected $p < 0.05$). The expression of *MPC1* was significantly upregulated in the cholesterogenic group in KIRC, LGG, lung adenocarcinoma (LUAD) and LUSC, and the

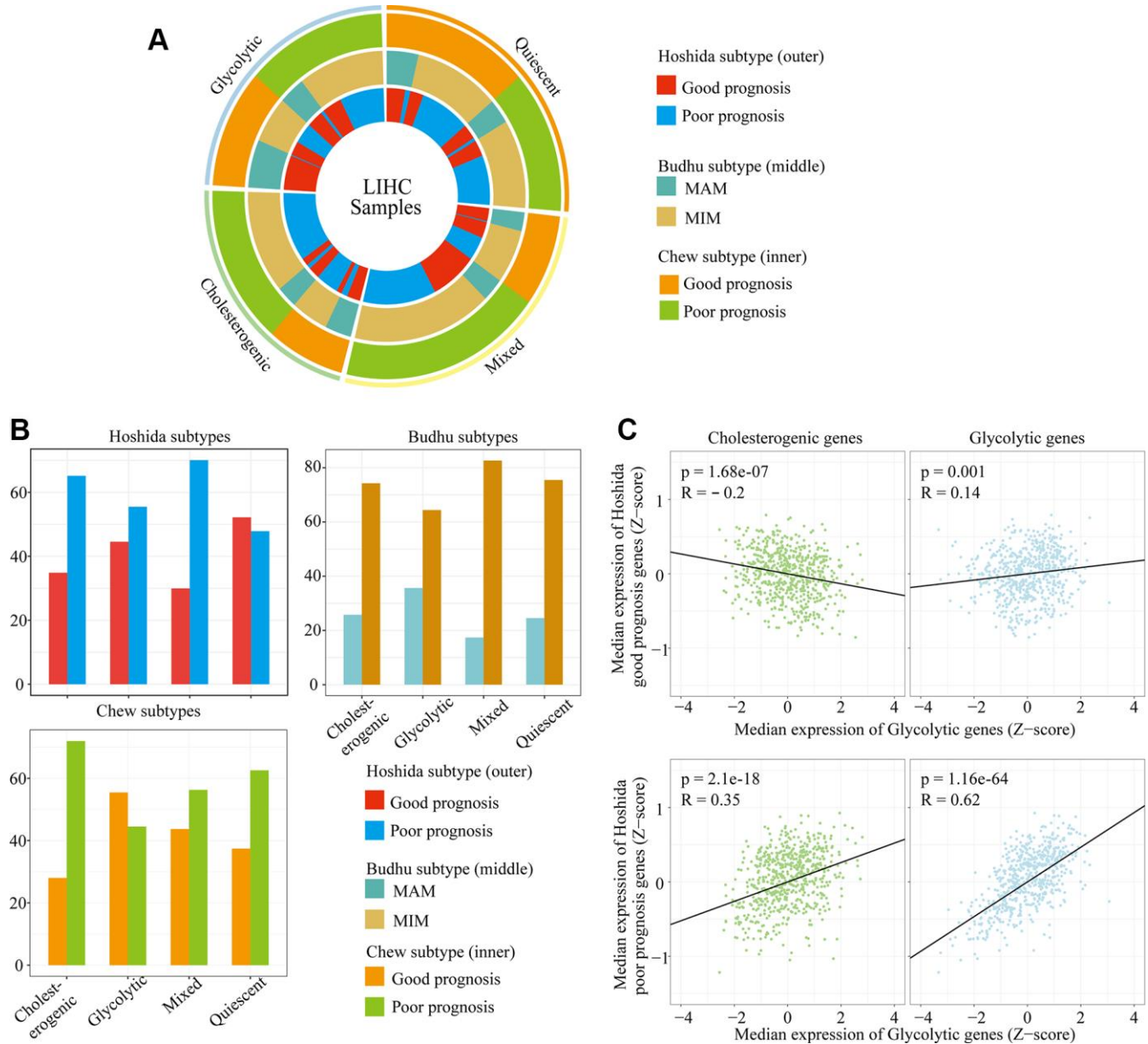


Figure 3. The alignment of LIHC metabolic subgroups with known gene expression subtypes. (A) Overlay of the metabolic gene profiles with LIHC expression subtypes based on the known classifications of Hoshida et al., Budhu et al. and Chew et al. **(B)** Bar plots of the proportion of LIHC expression subtypes in each metabolic subgroup. **(C)** Scatter plots depicting the correlations of glycolytic and cholesterogenic gene levels with prognostic gene levels in the Hoshida classification.

expression of *MPC2* was significantly upregulated in the cholesterogenic group in PAAD, sarcoma (SARC) and CESC (Figure 5B), similar to our findings in HCC. Further research is needed to explore the mRNA levels of these genes.

The potential associations between specific metabolic genes and the clinical features of various cancers were analyzed. The survival rates differed significantly among patients in the four metabolic subtypes in CESC ($p = 0.001$) (Figure 5C) and KIRC ($p < 0.001$) (Figure 5D). In CESC, the overall survival rate was significantly lower in the mixed subgroup than in the cholesterogenic group. In KIRC, the prognosis was worse in the glycolytic and quiescent groups than in the mixed and cholesterogenic groups. Thus, our model has provided novel insights into the molecular features of multiple cancers and revealed the tumor specificity of metabolic subtype gene expression.

DISCUSSION

HCC is a heterogeneous cancer that lacks effective treatment methods. Metabolic gene assessment may be a useful tool for investigating the metabolic abnormalities that characterize cancer cells [29]. During tumorigenesis, metabolic pathways are often reorganized to adapt to malignancy, and the corresponding tumor microenvironment contributes significantly to cancer progression. A relatively high proportion of malignant tumor tissues exhibit increased glycolytic properties, including HCC [30]. Che et al. reported that cholesterol synthesis accelerated cholesterol ester production and reduced triglyceride levels, thus accelerating hepatocarcinogenesis [31]. Highly expressed metabolic genes in HCC may accelerate metabolic dysfunction and tumorigenicity [32]. Therefore, elucidating the relevant metabolic pathways in HCC is crucial for prevention and treatment.

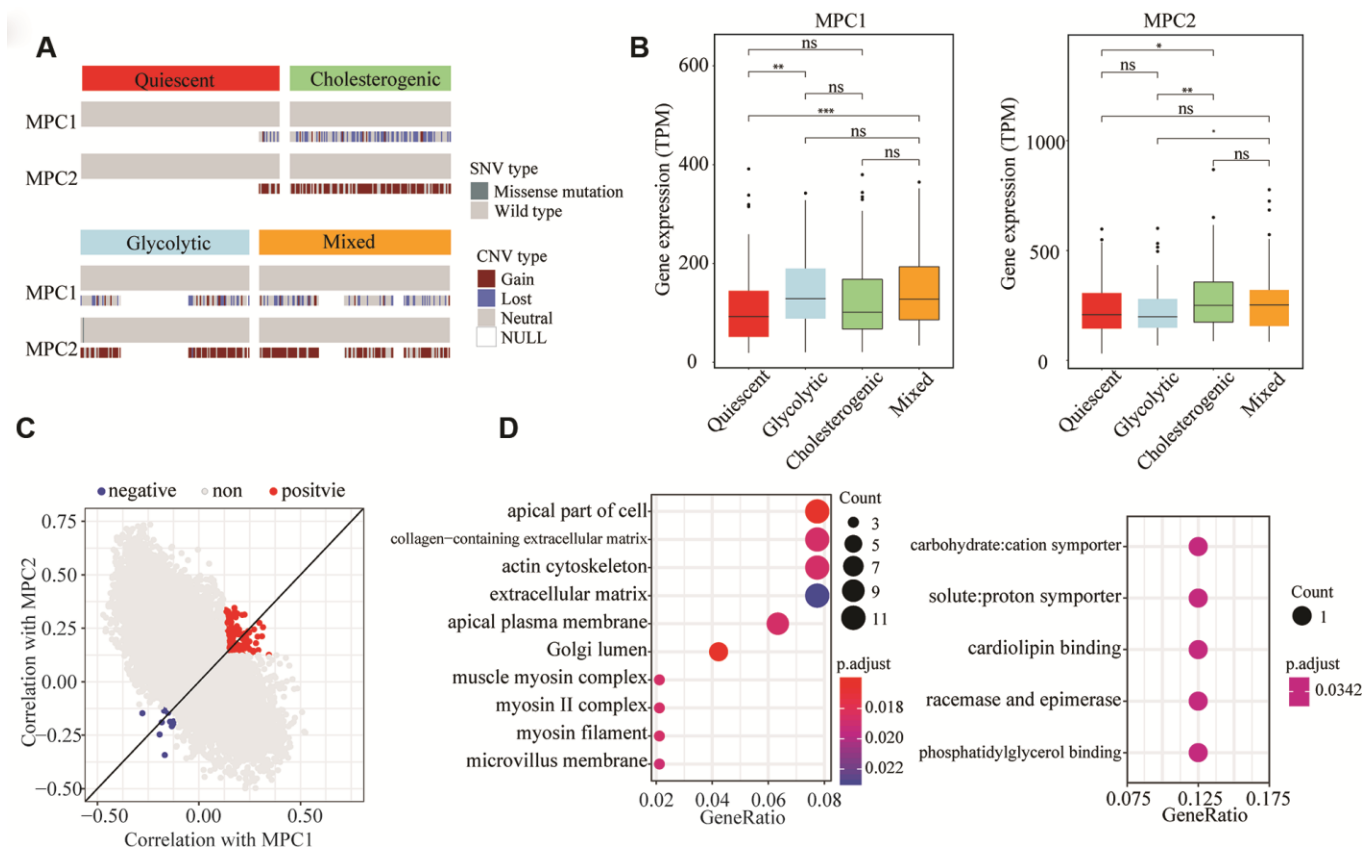


Figure 4. Association of *MPC1* and *MPC2* expression with LIHC metabolic subgroups and cell signaling pathways. (A) Oncoprint indicating the distribution of *MPC1* and *MPC2* SNVs and CNVs across the metabolic groups. Only one case was found with an SNV in *MPC2*. (B) Box plots of significant ($p < 0.001$) differences in *MPC1* and *MPC2* levels across the LIHC metabolic subgroups. (C) Scatter plot of the correlations of 25,483 genes with *MPC1* (x-axis) and *MPC2* (y-axis). In total, 168 genes correlated positively (Spearman correlation BH-adjusted $p < 0.01$) with both *MPC1* and *MPC2*, while 14 genes correlated negatively with both *MPC1* and *MPC2* (adjusted $p < 0.01$). (D) The most significantly enriched (hypergeometric test BH-adjusted $p < 0.05$) gene sets among the genes positively (left) and negatively (right) associated with *MPC1/2* expression.

Metabolic reprogramming studies have been conducted on glycolysis and the tricarboxylic acid cycle [33]. Many metabolic pathways occur in tumor cells, including fatty acid, glutamine, serine and cholesterol metabolism [34]. Numerous key enzymes in glycolysis are significantly upregulated in ovarian, pancreatic, breast and prostate cancer, as well as in osteosarcoma and melanoma [35]. Understanding the metabolic pathways that are disrupted in cancer can help researchers predict potentially responsible cells in tumor samples and gain insight into the disease etiology. For instance, Bénéteau et al. illustrated that inhibiting glycolysis could transform conventional tolerogenic cancer cells into immunogenic ones, thus providing a novel approach for immunogenic chemotherapy [36]. In the present study, we sought to establish a metabolic classification of HCC. Four specific subgroups were identified based on glycolytic

and cholesterogenic pathways that significantly influenced survival.

Glycolysis promotes tumor progression, immune escape and drug resistance. Glycolysis can reduce dependence on oxygen and replenish tumor cells quickly. The intermediate products of glycolysis can be transferred to the pentose phosphate pathway and other pathways for protein, nucleic acid and lipid synthesis to meet the anabolic and metabolic requirements for rapid tumor cell proliferation [37]. Active glycolysis can reduce the permeability of the outer membrane of the mitochondria, allowing tumor cells to resist cell death [38]. Glycolysis produces large amounts of lactic acid, resulting in an acidic environment that is conducive to tumor invasion and immune escape [39]. Tumor glycolysis is associated with changes in intracellular signaling pathways

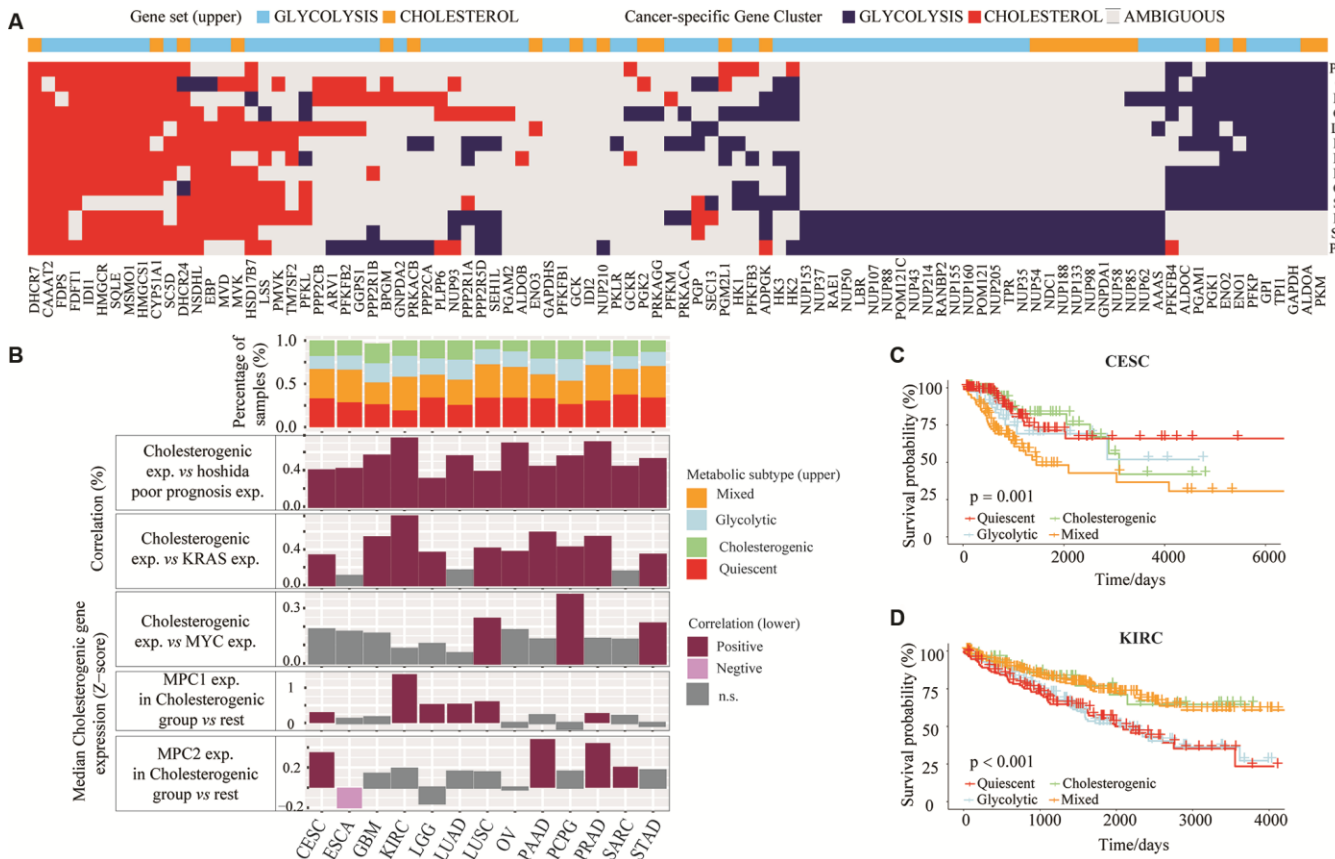


Figure 5. The glycolytic and cholesterogenic gene profiles of other cancer types. (A) Heat map depicting that glycolytic and cholesterogenic genes were robustly co-expressed when consensus clusters were applied to each individual cancer type. (B) Top: Bar plots showing the proportions of the metabolic subgroups across the various cancer types. Bottom: The correlation between cholesterogenic gene expression and the expression of Hoshida poor prognostic genes, *KRAS*, *MYC* and *MPC1/2* in each cancer type. Median glycolytic gene expression correlated positively (BH-adjusted $p < 0.05$) with basal-like gene expression in all cancer types. The correlation between *MPC1/2* expression and glycolytic gene expression was validated using Wilcoxon rank sum tests and BH correction. (C) Kaplan-Meier survival analysis curves depicting the differences in median overall survival across the metabolic subgroups in CESC. (D) Kaplan-Meier survival analysis curves demonstrating the differences in median overall survival in KIRC.

induced by a variety of oncogenic and/or tumor-suppressor genes. For example, the long non-coding RNA Ftx was found to promote aerobic glycolysis and tumor aggression by inducing the PPAR γ pathway in HCC [40]. Interestingly, in our study, the HCC subtype with higher glycolytic gene expression but lower cholesterologenic gene expression seemed to be both aggressive and sensitive to chemotherapy, as we observed survival benefits in this subgroup. Our results suggest that there are multiple metabolic phenotypes associated with glycolysis and cholesterol synthesis in HCC.

The liver is an important site of lipid metabolism, and cholesterol levels rise significantly in liver cancer cells. The activation of extracellular signal-regulated kinase in liver cells can inhibit the expression of the rate-limiting enzyme in cholesterol metabolism, thus inhibiting bile acid synthesis and inducing cholesterol accumulation [41]. Cholesterol metabolites or intermediates have been reported to promote the growth of cancer cells [42]. We confirmed the involvement of cholesterologenesis in the progression and classification of HCC by demonstrating that cholesterol synthesis genes were highly expressed in the tumor tissues of some patients and were associated with a poorer prognosis. Previous reports have indicated that statins suppress proliferation and induce apoptosis in HCC cells and improve the prognosis of HCC patients [43, 44], further illustrating the influence of metabolic reprogramming on HCC tumorigenesis.

We found that cholesterologenic gene expression correlated negatively with *TP53* expression and positively with *MYC* expression. Thus, abnormal expression of *TP53* and *MYC* may promote the malignant process of tumors by enhancing cholesterol synthesis and altering cholesterol use. In addition, by detecting mutated genes in metabolic pathways, we found that the MPC complexes regulating pyruvate flux were mutated and abnormally expressed in HCC, suggesting that changes in MPC are associated with HCC progression.

It is important to note that the correlation between glycolysis and cholesterol synthesis has been validated in various cancers. Our in-depth investigation demonstrated that the mutation of different metabolic genes and the expression of specific enzymes contribute to the unique metabolic characteristics and clinical prognoses of different cancer types. HCC metabolic typing based on metabolic reprogramming may provide important information to enable clinicians to select treatments, predict the potential response, anticipate treatment resistance and foresee the likely outcomes. Activating or inhibiting particular metabolic pathways may be a useful therapeutic strategy to prevent HCC progression.

MATERIALS AND METHODS

HCC dataset acquisition and processing

The HCC datasets and all corresponding clinical data were downloaded from the data portal of TCGA (Illumina HiSeq Systems; <https://cancergenome.nih.gov/>) and the ICGC (<https://www.icgc.org>) [45]. We also downloaded standardized RNA sequence data for all 423 available cases from TCGA and for 237 samples from the ICGC data portal. We used human genome reference sequence GRCh37 from the Genome Reference Consortium [46]. Samples from the ICGC were filtered to exclude those labeled as cell lines, xenografts, metastatic, normal or non-laser microscopy enrichment. After excluding these samples, we downloaded somatic mutational data (CNVs, SNVs and indexes) for all the screened samples.

Analysis of RNA sequence data

We normalized the RNA levels in each sample using the Transcripts Per Million algorithm and log-transformed $\log_{10}((\text{normalized count} * 1e^{6145}) + 1)$. To identify significantly differentially expressed RNAs, we used a standard screen of a \log_2 fold change ≥ 1 . All samples were screened to exclude those with tumor contents $< 30\%$ [47].

Batch profile estimation and correction

We analyzed data from TCGA and ICGC cohorts, applied a normalization strategy and removed unwanted variation as a correction. Batch corrections were performed in each cohort using a gene localization scale (Figure 6).

Classification of metabolic gene subgroups

The Molecular Signatures Database is critical for insightful interpretation of large-scale genomic data [48]. We used the "REACTOME GLYCOLYSIS" (n = 29) to identify the glycolytic subgroup and the "REACTOME CHOLESTEROL BIOSYNTHESIS" (n = 72) to identify the cholesterologenic subgroup. Subtypes were separated based on the consistent clustering of glycolytic and cholesterol-generating genes in ConsensusClusterPlus v1.38, and their statistical significance was assessed with SigClust (parameters: 160 reps=100, p Item=0.8, p Feature=1) [49]. Ward.D2 and the Euclidean distance were respectively used as clustering algorithms and distance measurements (k = 5 for glycolytic and cholesterologenic genes in resected and metastatic LIHC samples [n = 610], the cluster1]), and clusters 1-5 were validated. All patients were divided into four groups based on the

median levels of glycolytic and cholesterol-generating genes in each sample: the quiescent group (GLYCOLYSIS \leq 0, CHOLESTEROL \leq 0), the glycolytic group (GLYCOLYSIS $>$ 0, CHOLESTEROL \leq 0), the cholesterogenic group (GLYCOLYSIS \leq 0, CHOLESTEROL $>$ 0) and the mixed group (GLYCOLYSIS $>$ 0, CHOLESTEROL $>$ 0). For each gene cluster, the ratio of glycolytic genes and cholesterol-generating genes was calculated. Gene clusters containing $>$ 90% CHOLESTEROL genes or $>$ 30% GLYCOLYSIS genes were considered as “core” gene clusters.

Classification of pre-existing HCC subgroups

Consistent clustering was applied to classify samples based on the common tumor subtypes studied by Hoshida et al. [50], Budhu et al. [51] and Chew et al. [52]. The Hoshida subgrouping was based on the 186 genetic characteristics in the original publication, the Budhu subtyping was based on the 17 genetic characteristics in the original paper, and the Chew subtyping was based on the 14 genes in the original study. During each subtype classification, the samples were consistently clustered based on the genes of each classifier, and then semi-automatic subtype assignment was applied.

RNA expression analysis of *MPC1/2*

We used RNA-seq data to identify gene sets that correlated positively or negatively with *MPC1/2* (Spearman correlation analysis), and performed BH correction for multiple test corrections. A significant correlation was established between two gene sets based on an adjusted p value $<$ 0.01. A correlation coefficient

of $r >$ 0 was used to establish a positive correlation of a gene with *MPC1/2*, while a correlation coefficient of $r <$ 0 was used to establish a negative correlation. To determine the pathway enrichment of genes that correlated positively and negatively with *MPC1/2*, we performed a comprehensive gene set enrichment analysis on the two sets of genes.

Calculation of tumor content

The purity of each tumor sample was limited due to the presence of various immune cells surrounding the tumor cells, as well as other cells in the tumor microenvironment. We estimated the tumor purity of the HCC samples using an R package.

Mutation analysis of HCC genes

We identified and analyzed gene sequences from the human genome assembly GRCh37/hg19 [53]. In order to identify oncogenic molecular events in the HCC metabolic subtypes, we investigated the frequency of SNVs, INDELS and CNVs in commonly mutated HCC genes [54] and explored their relationship with the HCC metabolic subtypes. With respect to tumor ploidy, DNA fragments with copy statuses \geq 3 and \leq 1 were considered amplified and deleted, respectively. Based on a previous study [55], we screened HCC copy number events with at least 10 support probes and fragment averages $>$ 0.2 (amplified) or $<$ -0.2 (deleted). The coordinates of the copy number events were mapped to the gene coding region with Bedtools v2.26, and the SNVs and CNVs of each gene were tested with a contingency analysis. The selected genes in each subgroup were tested, and Fisher’s exact test was used to determine whether there was a loss-of-function

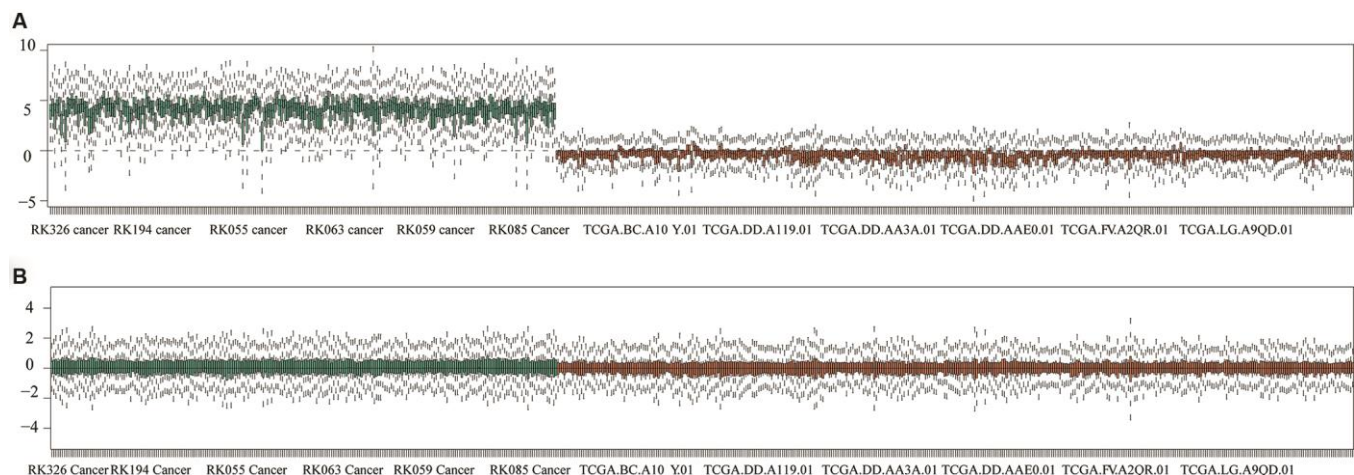


Figure 6. Batch correction of queued datasets from TCGA and ICGC. (A) Gene datasets were validated before normalization. **(B)** Gene datasets were illustrated after normalization.

mutation or copy number amplification/deletion in each subgroup. BH correction was applied to the resulting p values.

Pan-cancer RNA-seq analysis

We downloaded the Transcripts Per Million data of all pan-cancer samples and screened the samples according to cancer type. There were at least 100 samples after the preliminary screening, and there were 26 matched cancer types. Logarithmic conversion, batch correction, grouping and cluster analysis of RNA expression values were performed as described above. For each gene cluster, we calculated the ratio of glycolytic and cholesterol-generating genes. Gene clusters containing > 90% cholesterologenic genes or > 30% glycolytic genes were considered as “core” gene clusters. For cancer types with multiple core clusters in the same gene set, the most homogeneous cluster was considered to be the core cluster. Cancer types that did not have at least 75% homogeneous core glycolytic and cholesterologenic clusters were omitted from further analyses (specifically: bladder urothelial carcinoma, breast invasive carcinoma, colon adenocarcinoma, head and neck squamous cell carcinoma, kidney renal papillary cell carcinoma, acute myeloid leukemia, rectum adenocarcinoma, skin cutaneous melanoma, testicular germ cell tumors, thyroid carcinoma, thymoma and uterine corpus endometrial carcinoma (Supplementary Figure 1)). The metabolic subtypes of patients with each cancer type were determined based on the median values of the respective core glycolytic and cholesterol-generating genes.

Survival analysis of HCC patients

Kaplan-Meier diagrams were generated using the R packages "survival" v.2.4.2 and "survminer" v.0.4.2 [56]. Patients with a total survival of less than one month were removed from the survival analysis.

Statistical analysis

We used SPSS 23.0 software (IBM Corp., Armonk, NY, USA) and GraphPad Prism 7 (San Diego, CA, USA) to analyze the data [57]. Pearson correlation coefficients were used to express the linear correlations between pairs of variables. Kaplan-Meier and log-rank tests were used to analyze patient survival. R Studio was used to obtain the best cut-off value for each gene and survival curve. Two-sided p values < 0.05 were considered significant.

Abbreviations

HCC: hepatocellular carcinoma; TCGA: The Cancer Genome Atlas; ICGC: International Cancer Genome

Consortium; SNVs: single nucleotide variations; CNVs: copy number variations; LIHC: liver hepatocellular carcinoma; BH: Benjamini-Hochberg; CESC: cervical squamous cell carcinoma; GBM: glioblastoma multiforme; KIRC: kidney renal clear cell carcinoma; LGG: brain lower grade glioma; LUAD: lung adenocarcinoma; LUSC: lung squamous cell carcinoma; OV: ovarian serous cystadenocarcinoma; PAAD: pancreatic adenocarcinoma; PCPG: pheochromocytoma and paraganglioma; PRAD: prostate adenocarcinoma; STAD: stomach adenocarcinoma; SARC: sarcoma.

AUTHOR CONTRIBUTIONS

All of the authors worked collaboratively on the work presented here. JWJ and SSZ defined the research theme and discussed the analyses. QXZ, WWZ, XHC, HFL, DYC and ZH analyzed the data and drafted the manuscript. MS and LZ helped with the statistical analysis and reference collection. All authors read and approved the final manuscript.

ACKNOWLEDGMENTS

We thank the patients and investigators who participated in TCGA and ICGC for providing data.

CONFLICTS OF INTEREST

The authors have no conflicts of interest to report.

FUNDING

This study was supported by funds from the National Natural Science Foundation of China (81672422 and 81874038); the Open Project in the State Key Laboratory for Diagnosis and Treatment of Infectious Disease (2015KF03); the Zhejiang Province Health Department Program (2017KY322) and the National S&T Major Project of China (2018ZX10301201).

REFERENCES

1. Chen L, Guo P, He Y, Chen Z, Chen L, Luo Y, Qi L, Liu Y, Wu Q, Cui Y, Fang F, Zhang X, Song T, Guo H. HCC-derived exosomes elicit HCC progression and recurrence by epithelial-mesenchymal transition through MAPK/ERK signalling pathway. *Cell Death Dis.* 2018; 9:513. <https://doi.org/10.1038/s41419-018-0534-9> PMID:29725020
2. Lévy L, Renard CA, Wei Y, Buendia MA. Genetic alterations and oncogenic pathways in hepatocellular carcinoma. *Ann N Y Acad Sci.* 2002; 963:21–36. <https://doi.org/10.1111/j.1749-6632.2002.tb04091.x>

- PMID:[12095925](https://pubmed.ncbi.nlm.nih.gov/12095925/)
3. Law CT, Wei L, Tsang FH, Chan CY, Xu IM, Lai RK, Ho DW, Lee JM, Wong CC, Ng IO, Wong CM. HELLS Regulates Chromatin Remodeling and Epigenetic Silencing of Multiple Tumor Suppressor Genes in Human Hepatocellular Carcinoma. *Hepatology*. 2019; 69:2013–30.
<https://doi.org/10.1002/hep.30414>
PMID:[30516846](https://pubmed.ncbi.nlm.nih.gov/30516846/)
 4. He Y, Dang Q, Li J, Zhang Q, Yu X, Xue M, Guo W. Prediction of hepatocellular carcinoma prognosis based on expression of an immune-related gene set. *Aging (Albany NY)*. 2020; 12:965–77.
<https://doi.org/10.18632/aging.102669>
PMID:[31929113](https://pubmed.ncbi.nlm.nih.gov/31929113/)
 5. Wu S, Du R, Gao C, Kang J, Wen J, Sun T. The role of XBP1s in the metastasis and prognosis of hepatocellular carcinoma. *Biochem Biophys Res Commun*. 2018; 500:530–37.
<https://doi.org/10.1016/j.bbrc.2018.04.033>
PMID:[29627568](https://pubmed.ncbi.nlm.nih.gov/29627568/)
 6. Eason K, Sadanandam A. Molecular or metabolic reprogramming: what triggers tumor subtypes? *Cancer Res*. 2016; 76:5195–200.
<https://doi.org/10.1158/0008-5472.CAN-16-0141>
PMID:[27635042](https://pubmed.ncbi.nlm.nih.gov/27635042/)
 7. Sukumar M, Kishton RJ, Restifo NP. Metabolic reprogramming of anti-tumor immunity. *Curr Opin Immunol*. 2017; 46:14–22.
<https://doi.org/10.1016/j.coi.2017.03.011>
PMID:[28412583](https://pubmed.ncbi.nlm.nih.gov/28412583/)
 8. Strickland M, Stoll EA. Metabolic reprogramming in glioma. *Front Cell Dev Biol*. 2017; 5:43.
<https://doi.org/10.3389/fcell.2017.00043>
PMID:[28491867](https://pubmed.ncbi.nlm.nih.gov/28491867/)
 9. Beyoğlu D, Imbeaud S, Maurhofer O, Bioulac-Sage P, Zucman-Rossi J, Dufour JF, Idle JR. Tissue metabolomics of hepatocellular carcinoma: tumor energy metabolism and the role of transcriptomic classification. *Hepatology*. 2013; 58:229–38.
<https://doi.org/10.1002/hep.26350>
PMID:[23463346](https://pubmed.ncbi.nlm.nih.gov/23463346/)
 10. Liu KT, Yeh IJ, Chou SK, Yen MC, Kuo PL. Regulatory mechanism of fatty acid-CoA metabolic enzymes under endoplasmic reticulum stress in lung cancer. *Oncol Rep*. 2018; 40:2674–82.
<https://doi.org/10.3892/or.2018.6664>
PMID:[30132556](https://pubmed.ncbi.nlm.nih.gov/30132556/)
 11. Li C, He C, Xu Y, Xu H, Tang Y, Chavan H, Duan S, Artigues A, Forrest ML, Krishnamurthy P, Han S, Holzbeierlein JM, Li B. Alternol eliminates excessive ATP production by disturbing krebs cycle in prostate cancer. *Prostate*. 2019; 79:628–39.
<https://doi.org/10.1002/pros.23767>
PMID:[30663084](https://pubmed.ncbi.nlm.nih.gov/30663084/)
 12. Linehan WM, Ricketts CJ. The metabolic basis of kidney cancer. *Semin Cancer Biol*. 2013; 23:46–55.
<https://doi.org/10.1016/j.semcancer.2012.06.002>
PMID:[22705279](https://pubmed.ncbi.nlm.nih.gov/22705279/)
 13. Han X, Zheng T, Foss FM, Lan Q, Holford TR, Rothman N, Ma S, Zhang Y. Genetic polymorphisms in the metabolic pathway and non-hodgkin lymphoma survival. *Am J Hematol*. 2010; 85:51–56.
<https://doi.org/10.1002/ajh.21580> PMID:[20029944](https://pubmed.ncbi.nlm.nih.gov/20029944/)
 14. Xue C, He Y, Zhu W, Chen X, Yu Y, Hu Q, Chen J, Liu L, Ren F, Ren Z, Cui G, Sun R. Low expression of LACTB promotes tumor progression and predicts poor prognosis in hepatocellular carcinoma. *Am J Transl Res*. 2018; 10:4152–62.
PMID:[30662658](https://pubmed.ncbi.nlm.nih.gov/30662658/)
 15. Xu F, Yan JJ, Gan Y, Chang Y, Wang HL, He XX, Zhao Q. miR-885-5p negatively regulates warburg effect by silencing hexokinase 2 in liver cancer. *Mol Ther Nucleic Acids*. 2019; 18:308–19.
<https://doi.org/10.1016/j.omtn.2019.09.002>
PMID:[31614321](https://pubmed.ncbi.nlm.nih.gov/31614321/)
 16. Baulies A, Montero J, Matías N, Insausti N, Terrones O, Basañez G, Vallejo C, Conde de La Rosa L, Martinez L, Robles D, Morales A, Abian J, Carrascal M, et al. The 2-oxoglutarate carrier promotes liver cancer by sustaining mitochondrial GSH despite cholesterol loading. *Redox Biol*. 2018; 14:164–77.
<https://doi.org/10.1016/j.redox.2017.08.022>
PMID:[28942194](https://pubmed.ncbi.nlm.nih.gov/28942194/)
 17. Zhang Y, Zhao Y, Cai EB, Gao YG, Zhong-Mei HE, Yang H, Liu SL, Zhang LX. [Research progress on structural modification and bioactivities of cholesterol.] *Journal of Food Safety & Quality*. 2016; 7:693–700.
 18. Peng X, Chen Z, Farshidfar F, Xu X, Lorenzi PL, Wang Y, Cheng F, Tan L, Mojumdar K, Du D, Ge Z, Li J, Thomas GV, et al, and Cancer Genome Atlas Research Network. Molecular characterization and clinical relevance of metabolic expression subtypes in human cancers. *Cell Rep*. 2018; 23:255–269.e4.
<https://doi.org/10.1016/j.celrep.2018.03.077>
PMID:[29617665](https://pubmed.ncbi.nlm.nih.gov/29617665/)
 19. Murray B, Barbier-Torres L, Fan W, Mato JM, Lu SC. Methionine adenosyltransferases in liver cancer. *World J Gastroenterol*. 2019; 25:4300–4319.
<https://doi.org/10.3748/wjg.v25.i31.4300>
PMID:[31496615](https://pubmed.ncbi.nlm.nih.gov/31496615/)
 20. Liu H, Luo J, Luan S, He C, Li Z. Long non-coding RNAs involved in cancer metabolic reprogramming. *Cell Mol Life Sci*. 2019; 76:495–504.

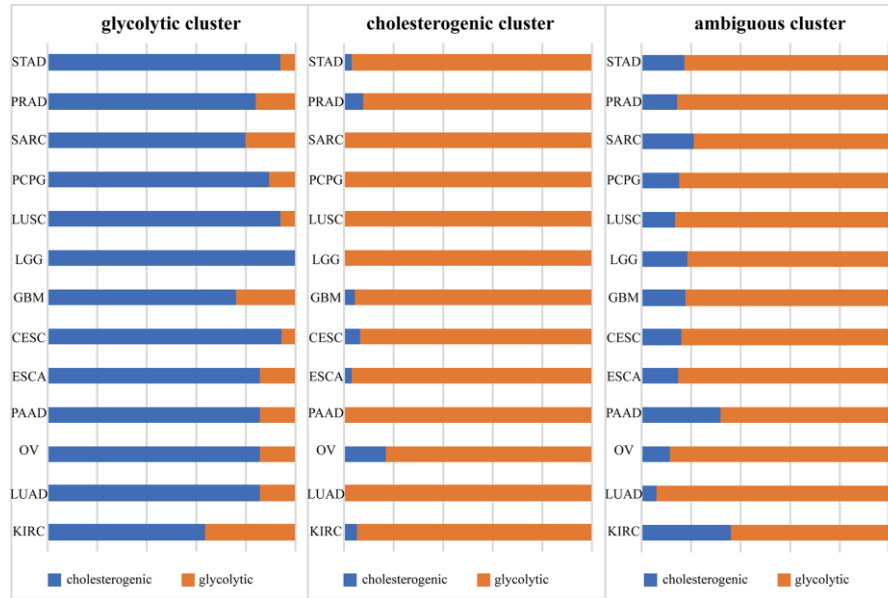
- <https://doi.org/10.1007/s00018-018-2946-1>
PMID:[30341461](https://pubmed.ncbi.nlm.nih.gov/30341461/)
21. Lévy P, Bartosch B. Metabolic reprogramming: A hallmark of viral oncogenesis. *Oncogene*. 2016; 35:4155–64.
<https://doi.org/10.1038/onc.2015.479>
PMID:[26686092](https://pubmed.ncbi.nlm.nih.gov/26686092/)
22. Bailey P, Chang DK, Nones K, Johns AL, Patch AM, Gingras MC, Miller DK, Christ AN, Bruxner TJ, Quinn MC, Nourse C, Murtaugh LC, Harliwong I, et al, and Australian Pancreatic Cancer Genome Initiative. Genomic analyses identify molecular subtypes of pancreatic cancer. *Nature*. 2016; 531:47–52.
<https://doi.org/10.1038/nature16965>
PMID:[26909576](https://pubmed.ncbi.nlm.nih.gov/26909576/)
23. Chen X, Cheung ST, So S, Fan ST, Barry C, Higgins J, Lai KM, Ji J, Dudoit S, Ng IO, Van De Rijn M, Botstein D, Brown PO. Gene expression patterns in human liver cancers. *Mol Biol Cell*. 2002; 13:1929–39.
<https://doi.org/10.1091/mbc.02-02-0023>
PMID:[12058060](https://pubmed.ncbi.nlm.nih.gov/12058060/)
24. Wu C, Hao YY, Xia J, Huang R, Wu YF, Zhang J, Qiu YD. 815 characteristics of T cell subsets and programmed death 1 expression on T cells in HBV-related hepatocellular carcinoma (HCC). *J Hepatol*. 2012; 56:S318–19.
[https://doi.org/10.1016/S0168-8278\(12\)60827-7](https://doi.org/10.1016/S0168-8278(12)60827-7)
25. Tompkins SC, Sheldon RD, Rauckhorst AJ, Noterman MF, Solst SR, Buchanan JL, Mapuskar KA, Pewa AD, Gray LR, Oonthonpan L, Sharma A, Scerbo DA, Dupuy AJ, et al. Disrupting mitochondrial pyruvate uptake directs glutamine into the TCA cycle away from glutathione synthesis and impairs hepatocellular tumorigenesis. *Cell Rep*. 2019; 28:2608–2619.e6.
<https://doi.org/10.1016/j.celrep.2019.07.098>
PMID:[31484072](https://pubmed.ncbi.nlm.nih.gov/31484072/)
26. Li X, Ji Y, Han G, Li X, Fan Z, Li Y, Zhong Y, Cao J, Zhao J, Zhang M, Wen J, Goscinski MA, Nesland JM, Suo Z. MPC1 and MPC2 expressions are associated with favorable clinical outcomes in prostate cancer. *BMC Cancer*. 2016; 16:894.
<https://doi.org/10.1186/s12885-016-2941-6>
PMID:[27852261](https://pubmed.ncbi.nlm.nih.gov/27852261/)
27. Ma X, Cui Y, Zhou H, Li Q. Function of mitochondrial pyruvate carriers in hepatocellular carcinoma patients. *Oncol Lett*. 2018; 15:9110–16.
<https://doi.org/10.3892/ol.2018.8466> PMID:[29805642](https://pubmed.ncbi.nlm.nih.gov/29805642/)
28. Hu J, Locasale JW, Bielas JH, O'Sullivan J, Sheahan K, Cantley LC, Vander Heiden MG, Vitkup D. Heterogeneity of tumor-induced gene expression changes in the human metabolic network. *Nat Biotechnol*. 2013; 31:522–29.
<https://doi.org/10.1038/nbt.2530>
PMID:[23604282](https://pubmed.ncbi.nlm.nih.gov/23604282/)
29. Lagziel S, Lee WD, Shlomi T. Inferring cancer dependencies on metabolic genes from large-scale genetic screens. *BMC Biol*. 2019; 17:37.
<https://doi.org/10.1186/s12915-019-0654-4>
PMID:[31039782](https://pubmed.ncbi.nlm.nih.gov/31039782/)
30. Shibao S, Minami N, Koike N, Fukui N, Yoshida K, Saya H, Sampetean O. Metabolic heterogeneity and plasticity of glioma stem cells in a mouse glioblastoma model. *Neuro Oncol*. 2018; 20:343–54.
<https://doi.org/10.1093/neuonc/nox170>
PMID:[29016888](https://pubmed.ncbi.nlm.nih.gov/29016888/)
31. Che L, Chi W, Qiao Y, Zhang J, Song X, Liu Y, Li L, Jia J, Pilo MG, Wang J, Cigliano A, Ma Z, Kuang W, et al. Cholesterol biosynthesis supports the growth of hepatocarcinoma lesions depleted of fatty acid synthase in mice and humans. *Gut*. 2020; 69:177–86.
<https://doi.org/10.1136/gutjnl-2018-317581>
PMID:[30954949](https://pubmed.ncbi.nlm.nih.gov/30954949/)
32. Tian Y, Yang B, Qiu W, Hao Y, Zhang Z, Yang B, Li N, Cheng S, Lin Z, Rui YC, Cheung OK, Yang W, Wu WK, et al. ER-residential nogo-B accelerates NAFLD-associated HCC mediated by metabolic reprogramming of oxLDL lipophagy. *Nat Commun*. 2019; 10:3391.
<https://doi.org/10.1038/s41467-019-11274-x>
PMID:[31358770](https://pubmed.ncbi.nlm.nih.gov/31358770/)
33. Parekh LJ. Studies on some of the enzymes of glycolysis and tricarboxylic acid cycle and glutamic acid metabolism in the excised roots of *P. Mungo* L. *Enzymologia*. 1970; 38:9–18.
PMID:[5417471](https://pubmed.ncbi.nlm.nih.gov/5417471/)
34. Papathanassiou AE, Ko JH, Imprialou M, Bagnati M, Srivastava PK, Vu HA, Cucchi D, McAdoo SP, Ananieva EA, Mauro C, Behmoaras J. BCAT1 controls metabolic reprogramming in activated human macrophages and is associated with inflammatory diseases. *Nat Commun*. 2017; 8:16040.
<https://doi.org/10.1038/ncomms16040>
PMID:[28699638](https://pubmed.ncbi.nlm.nih.gov/28699638/)
35. Warmoes MO, Locasale JW. Heterogeneity of glycolysis in cancers and therapeutic opportunities. *Biochem Pharmacol*. 2014; 92:12–21.
<https://doi.org/10.1016/j.bcp.2014.07.019>
PMID:[25093285](https://pubmed.ncbi.nlm.nih.gov/25093285/)
36. Bénétteau M, Zunino B, Jacquin MA, Meynet O, Chiche J, Pradelli LA, Marchetti S, Cornille A, Carles M, Ricci JE. Combination of glycolysis inhibition with chemotherapy results in an antitumor immune response. *Proc Natl Acad Sci USA*. 2012; 109:20071–76.
<https://doi.org/10.1073/pnas.1206360109>
PMID:[23169636](https://pubmed.ncbi.nlm.nih.gov/23169636/)

37. Feng Y, Zhang Y, Cai Y, Liu R, Lu M, Li T, Fu Y, Guo M, Huang H, Ou Y, Chen Y. A20 targets PFKL and glycolysis to inhibit the progression of hepatocellular carcinoma. *Cell Death Dis.* 2020; 11:89. <https://doi.org/10.1038/s41419-020-2278-6> PMID:32015333
38. Lee AC, Zizi M, Colombini M. beta-NADH decreases the permeability of the mitochondrial outer membrane to ADP by a factor of 6. *J Biol Chem.* 1994; 269:30974–80. PMID:7983033
39. Abaza M, Luqmani YA. The influence of pH and hypoxia on tumor metastasis. *Expert Rev Anticancer Ther.* 2013; 13:1229–42. <https://doi.org/10.1586/14737140.2013.843455> PMID:24099530
40. Li X, Zhao Q, Qi J, Wang W, Zhang D, Li Z, Qin C. lncRNA Ftx promotes aerobic glycolysis and tumor progression through the PPAR γ pathway in hepatocellular carcinoma. *Int J Oncol.* 2018; 53:551–66. <https://doi.org/10.3892/ijo.2018.4418> PMID:29845188
41. Jones RD, Repa JJ, Russell DW, Dietschy JM, Turley SD. Delineation of biochemical, molecular, and physiological changes accompanying bile acid pool size restoration in Cyp7a1(-/-) mice fed low levels of cholic acid. *Am J Physiol Gastrointest Liver Physiol.* 2012; 303:G263–74. <https://doi.org/10.1152/ajpgi.00111.2012> PMID:22628034
42. Murtola TJ, Syväälä H, Pennanen P, Bläuer M, Solakivi T, Ylikomi T, Tammela TL. The importance of LDL and cholesterol metabolism for prostate epithelial cell growth. *PLoS One.* 2012; 7:e39445. <https://doi.org/10.1371/journal.pone.0039445> PMID:22761797
43. Goh MJ, Sinn DH, Kim S, Woo SY, Cho H, Kang W, Gwak GY, Paik YH, Choi MS, Lee JH, Koh KC, Paik SW. Statin use and the risk of hepatocellular carcinoma in patients with chronic hepatitis B. *Hepatology.* 2019. [Epub ahead of print]. <https://doi.org/10.1002/hep.30973> PMID:31556128
44. Kang H, Oh T, Bahk YY, Kim GH, Kan SY, Shin DH, Kim JH, Lim JH. HSF1 regulates mevalonate and cholesterol biosynthesis pathways. *Cancers (Basel).* 2019; 11:1363. <https://doi.org/10.3390/cancers11091363> PMID:31540279
45. He Y, Xue C, Yu Y, Chen J, Chen X, Ren F, Ren Z, Cui G, Sun R. CD44 is overexpressed and correlated with tumor progression in gallbladder cancer. *Cancer Manag Res.* 2018; 10:3857–65. <https://doi.org/10.2147/CMAR.S175681> PMID:30288117
46. Ramos A, Santos C, Barbena E, Mateiu L, Alvarez L, Nogués R, Aluja MP. Validated primer set that prevents nuclear DNA sequences of mitochondrial origin co-amplification: a revision based on the new human genome reference sequence (GRCh37). *Electrophoresis.* 2011; 32:782–83. <https://doi.org/10.1002/elps.201000583> PMID:21425173
47. Karasinska JM, Topham JT, Kalloger SE, Jang GH, Denroche RE, Culibrk L, Williamson LM, Wong HL, Lee MK, O’Kane GM, Moore RA, Mungall AJ, Moore MJ, et al. Altered gene expression along the glycolysis-cholesterol synthesis axis is associated with outcome in pancreatic cancer. *Clin Cancer Res.* 2020; 26:135–46. <https://doi.org/10.1158/1078-0432.CCR-19-1543> PMID:31481506
48. Liberzon A, Subramanian A, Pinchback R, Thorvaldsdóttir H, Tamayo P, Mesirov JP. Molecular signatures database (MSigDB) 3.0. *Bioinformatics.* 2011; 27:1739–40. <https://doi.org/10.1093/bioinformatics/btr260> PMID:21546393
49. Wilkerson MD, Hayes DN. ConsensusClusterPlus: a class discovery tool with confidence assessments and item tracking. *Bioinformatics.* 2010; 26:1572–73. <https://doi.org/10.1093/bioinformatics/btq170> PMID:20427518
50. Hoshida Y, Villanueva A, Kobayashi M, Peix J, Chiang DY, Camargo A, Gupta S, Moore J, Wrobel MJ, Lerner J, Reich M, Chan JA, Glickman JN, et al. Gene expression in fixed tissues and outcome in hepatocellular carcinoma. *N Engl J Med.* 2008; 359:1995–04. <https://doi.org/10.1056/NEJMoa0804525> PMID:18923165
51. Budhu A, Forgues M, Ye QH, Jia HL, He P, Zanetti KA, Kammula US, Chen Y, Qin LX, Tang ZY, Wang XW. Prediction of venous metastases, recurrence, and prognosis in hepatocellular carcinoma based on a unique immune response signature of the liver microenvironment. *Cancer Cell.* 2006; 10:99–111. <https://doi.org/10.1016/j.ccr.2006.06.016> PMID:16904609
52. Chew V, Chen J, Lee D, Loh E, Lee J, Lim KH, Weber A, Slinkamenac K, Poon RT, Yang H, Ooi LL, Toh HC, Heikenwalder M, et al. Chemokine-driven lymphocyte infiltration: an early intratumoural event determining long-term survival in resectable hepatocellular carcinoma. *Gut.* 2012; 61:427–38. <https://doi.org/10.1136/gutjnl-2011-300509> PMID:21930732
53. Cadeddu M, Vargiu L, Rodriguez-Tomé P, Sperber GO, Blomberg J, Tramontano E. Identification and analysis

- of HML2 sequences in human genome assembly GRCh37/hg19. *Retrovirology*. 2013; 10:P9.
<https://doi.org/10.1186/1742-4690-10-S1-P9>
54. Duitama J, Quintero JC, Cruz DF, Quintero C, Hubmann G, Foulquié-Moreno MR, Verstrepen KJ, Thevelein JM, Tohme J. An integrated framework for discovery and genotyping of genomic variants from high-throughput sequencing experiments. *Nucleic Acids Res*. 2014; 42:e44.
<https://doi.org/10.1093/nar/gkt1381>
PMID:[24413664](https://pubmed.ncbi.nlm.nih.gov/24413664/)
55. Laddha SV, Ganesan S, Chan CS, White E. Mutational landscape of the essential autophagy gene BECN1 in human cancers. *Mol Cancer Res*. 2014; 12:485–90.
<https://doi.org/10.1158/1541-7786.MCR-13-0614>
PMID:[24478461](https://pubmed.ncbi.nlm.nih.gov/24478461/)
56. Therneau TM. Survival Analysis [R package survival version 2.39-5]. 2015.
<https://github.com/therneau/survival>
57. He Y, Chen X, Yu Y, Li J, Hu Q, Xue C, Chen J, Shen S, Luo Y, Ren F, Li C, Bao J, Yan J, et al. LDHA is a direct target of miR-30d-5p and contributes to aggressive progression of gallbladder carcinoma. *Mol Carcinog*. 2018; 57:772–83.
<https://doi.org/10.1002/mc.22799>
PMID:[29569755](https://pubmed.ncbi.nlm.nih.gov/29569755/)

SUPPLEMENTARY MATERIALS

Supplementary Figure



Supplementary Figure 1. Glycolysis- and cholesterol-related core gene clusters in 13 cancer types.

Supplementary Tables

Supplementary Table 1. Extent of various LIHC subtypes and metabolic phenotypes in each sample.

Row Labels	Count of Hoshiba_groups	Count of Budhu_groups	Count of Chew_groups
Cholesterogenic	132	132	132
Glycolytic	146	146	146
Mixed	167	167	167
Quiescent	163	163	163
Grand Total	608	608	608

Count of Chew_groups	Column Labels	Count of Chew_groups	Column Labels
Row Labels	Good	Poor	Grand Total
Cholesterogenic	37	95	132
Glycolytic	81	65	146
Mixed	73	94	167
Quiescent	61	102	163
Grand Total	252	356	608

Count of Budhu_groups	Column Labels	Count of Budhu_groups	Column Labels
Row Labels	Mam	Mim	Grand Total
Cholesterogenic	34	98	132
Glycolytic	52	94	146
Mixed	29	138	167
Quiescent	40	123	163
Grand Total	155	453	608

Count of Hoshiba_groups	Column Labels	Count of Hoshiba_groups	Column Labels
Row Labels	Good	Poor	Grand Total
Cholesterogenic	46	86	132
Glycolytic	65	81	146
Mixed	50	117	167
Quiescent	85	78	163
Grand Total	246	362	608

Row Labels	Good	Poor	<i>p</i> value
Cholesterogenic	28.03030303	71.969697	0.22701108
Glycolytic	55.47945205	44.520548	0.0156542
Mixed	43.71257485	56.2874252	0.38750472
Quiescent	37.42331288	62.5766871	

Row Labels	Mam	Mim	<i>p</i> value
Cholesterogenic	25.75757576	74.2424242	1
Glycolytic	35.61643836	64.3835616	0.12422132
Mixed	17.36526946	82.6347305	0.22402215
Quiescent	24.5398773	75.4601227	

Row Labels	Good	Poor	<i>p</i> value
Cholesterogenic	34.84848485	65.1515152	0.02223115
Glycolytic	44.52054795	55.4794521	0.39599375
Mixed	29.94011976	70.0598802	0.00243795
Quiescent	52.14723926	47.8527607	

Please browse Full Text version to see the data of Supplementary Table 2.

Supplementary Table 2. Consistent cluster analysis of glycolytic and cholesterogenic gene expression in 26 cancer types (tumor content \geq 30%).